



## VISUALIZATION OF FOREIGN GASES IN ATMOSPHERIC AIR

**Thomas C. Gruber Jr.\*, Larry B. Grim\***  
**\*MESH, Inc., 114 Barnsley Rd., Oxford, PA 19363**

**Keywords:** *infrared, spectrometer, tomography, cloud-tracking*

### ABSTRACT

*A Chemical Cloud Tracking System (CCTS) for monitoring foreign gas clouds (FGC) was developed. Path integrated concentration measurements from multiple synchronized-scanning passive infrared (IR) sensors are processed with a tomography algorithm to produce real-time cloud maps. The cloud size and motion are reported graphically. The CCTS technology, data reduction method, and a selected cloud map sequence are presented.*

### 1 INTRODUCTION

What's in the air ahead? In today's world the possibility of an attack from a rogue nation or a terrorist group using a colorless, odorless, poisonous gas must be considered. Whether the chemical release is on a battlefield or in a city, the identification of the gas and mapping of the cloud movement is best done at a distance. Infrared (IR) chemical sensors can detect, identify, and map hazardous gases from a safe distance. MESH, Inc. has developed two IR chemical sensor systems as a result of 15 years of R&D. These are the Mobile Chemical Agent Detector (MCAD) and the Chemical Cloud Tracking System (CCTS). These mobile platform and fixed site sensors locate foreign gas clouds (FGC) on a computer map display in real time. The MCAD is designed to detect nerve and blister agent chemical weapon vapors from vehicle-based platforms for military missions. The CCTS is designed to produce quantitative concentration maps of FGC releases that are used in chemical sensor field tests. Other potential CCTS applications include industrial site monitoring and large scale gas plume visualization research. The CCTS technology, data reduction, and typical results are discussed.

#### 1.1 Scanning Standoff Sensors

Unlike point sensors, IR spectrometer-based chemical sensors are called 'standoff' sensors because they do not need to come in direct contact with the gas cloud. The MCAD and CCTS have detection ranges up to 5 km. A single spectrometer-based chemical sensor can monitor an area as large as 80 km<sup>2</sup>, as long as a clear line-of-sight is available. Many point sensors would be required to cover an area of this size.

Each standoff sensor is mounted on a pan-and-tilt unit, which can point the sensor field of view (FOV) in a desired direction. The pan-and-tilt unit is automatically controlled to scan a desired field of regard (FOR), such as 360 degrees in azimuth by -2 to +10 degrees of elevation. The sensor data from scanning the FOR are used to map FGCs in real-time.

## 1.2 CCTS Development and Application

MESH, Inc. developed the CCTS for the West Desert Test Center (WDTC) at Dugway Proving Ground to support their chemical sensor field testing ‘ground truth’ requirements. Various types of standoff sensors and point sensors are tested by WDTC in open-air releases of approved vapors. The CCTS serves as a referee system for these releases by measuring the FGC size, location, and concentration in real-time. The CCTS consists of four sensors that are positioned on the corners of a 1 km x 1 km truth box. The data from the CCTS synchronized scanning sensors are fed through a tomography algorithm to produce real-time cloud maps. A fifth sensor in the CCTS monitors the maximum cloud height. The CCTS development was funded by phase I/phase II SBIRs and additional support/development contracts with WDTC.

## 2 CCTS VISUALIZATION TECHNOLOGY

The challenges of passive standoff chemical sensing and cloud mapping were solved during the past 15 years of R&D. These challenges included:

- Developing a low false positive detection algorithm,
- Developing methods for quantitative processing,
- Shrinking and automating the calibration device,
- Embedding the data acquisition and the computer electronics, and
- Developing real-time tomography/mapping software.

The solutions were engineered by a multidisciplinary team consisting of mechanical, electrical, and computer science engineers. The CCTS cloud visualization technology is discussed in the following sections.

### 2.1 Passive Sensing

The MCAD and CCTS sensors use Fourier transform infrared (FTIR) spectrometers. Most FTIR manufacturers focus on active FTIR. In active sensing, a high temperature blackbody source is used to illuminate an open-path region of interest between the FTIR and the source or to illuminate an extracted sample within a gas cell, i.e., a point sensor version of FTIR. This should not be confused with the passive FTIR used by the MCAD and CCTS. In passive FTIR, there is no artificial high-temperature IR source. Passive FTIR takes advantage of naturally existing temperature contrast between the FGC temperature and the effective background temperature. Temperature differences as small as 1 K are sufficient to detect and identify FGCs with features in the 7-14  $\mu\text{m}$  region of the IR. Although active FTIR achieves lower minimum detection limits, active FTIR cannot cover a 360 degree FOR because it is impractical to position blackbody sources in every direction of interest.

### 2.2 FTIR Spectrometer

FTIR spectrometers opto-mechanically take the Fourier transform of the incident scene radiance to produce an output signal called an interferogram (igram). This is accomplished by separating the scene radiance into two beams via a beam splitter, as shown in the Michelson FTIR schematic in Figure 1. These beams travel path distances of  $2L_1$  or  $2L_2$  before recombining at the beam splitter. The recombination is a constructive or destructive interference depending on the net phase difference between the beams. The net phase difference is proportional to the path difference of  $2(L_2 - L_1)$ ,

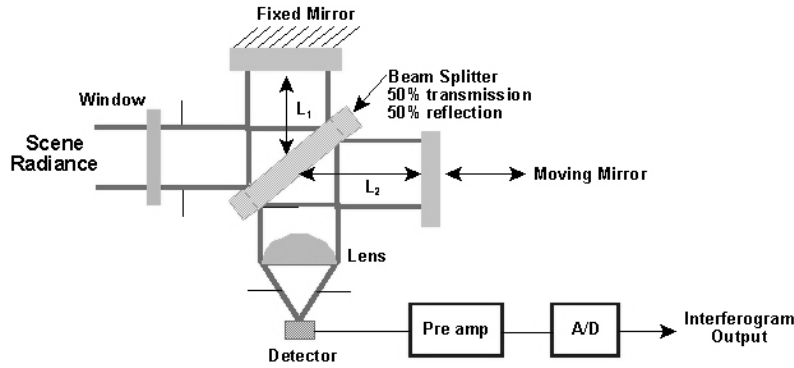


Fig. 1 – Michelson FTIR sensor schematic.

which is a function of the moving mirror position. The resulting igrum signal is detected with a cooled IR detector element, such as HgCdTe @ 80 K. The reciprocating mirror speed is proportional to the igrum rate. For CCTS sensors, the speed is set to produce 12 igrums per second. The moving mirror stroke length is proportional to the spectral resolution. The CCTS sensors are configured to collect 8 cm<sup>-1</sup> resolution igrums, which corresponds to a 0.125 cm stroke length.

The digitized igrum is processed with computer software that Fourier transforms the igrum to get back the measured spectrum. The spectrum is basically proportional to the scene radiance, which has units of power per unit area per solid angle per unit frequency. FTIR spectra are plotted as a function of wavenumber, which is related to frequency. The wavenumber,  $\nu$ , is related to the more familiar wavelength,  $\lambda$ , by:

$$\nu \text{ cm}^{-1} = ( 1 / (\lambda \mu\text{m})) ( 10000 \text{ cm}^{-1} \mu\text{m} ) \quad (1)$$

FTIR spectrometers usually have throughput and signal-to-noise ratio (SNR) advantages over grating, prism, and filter-based spectrometers, which directly measure the radiance for each wavenumber bin in the spectrum [1]. The SNR advantage is due to the multiplexing of all wavelengths in the igrum signal.

### 2.3 FTIRBox

The CCTS sensors, which are called FTIRBoxes, use a BLOCK Engineering FTIR spectrometer with a 1.5 degree FOV. The FTIR unit is repackaged with an embedded electronics stack, automated thermoelectric blackbody source, and environmental controls. The sensor is mounted on a Quickset pan and tilt unit to complete the sensor scanner assembly (SSA). A power and communication (POWCOM) interface box connects the SSA to the wireless Ethernet network and with a local power generator.

The embedded software acquires and processes FTIR sensor data, calibrates the FTIR sensor, and detects, identifies, and quantifies FGCs. The detection results are sent over the network to a command post for real time tomography processing and map display. The embedded electronics stack includes a flash disk for saving all the data including a log file and the igrum data file. The log file is useful for recording the status of the hardware and verifying successful operation of the system. The data file can be post processed to produce additional spectra files and other results depending on the user’s needs.

## 2.4 Signal Model

The FTIR sensor signal can be explained with the following simplified model [2]:

$$I_{\text{sensor}} = \tau I_o + (1 - \tau) I_a \quad (2)$$

where  $I_{\text{sensor}}$  is the net scene radiance incident on the sensor,  $\tau$  is the FGC transmission that contains the foreign gas's 'fingerprint',  $I_o$  is the background radiance, and  $I_a$  is the Planck radiance function evaluated at the ambient air temperature,  $T_a$ . All the radiance terms have units of  $\mu\text{W}/(\text{cm}^2 \text{sr cm}^{-1})$ . Each term in the model is a function of wavenumber. It is assumed that the ambient air and FGC temperatures are the same. The FGC attenuates the background radiance and the FGC emits radiance, as shown in Figure 2. As long as there is a small temperature difference,  $\Delta T$ , between the cloud and the effective background, then there are net absorption ( $T_a < T_o$ ) or net emission ( $T_a > T_o$ ) features in the spectrum due to the FGC. Natural backgrounds include low-angle sky, mountains, vegetation, urban environments, etc. All of these backgrounds emit IR light in the 7-14  $\mu\text{m}$  spectral region.

The FGC spectral features, i.e., fingerprint, are functions of the absorption coefficient spectrum, which is unique for each gaseous chemical, and the path integrated concentration, which is referred to as the concentration pathlength (CL). The L part of CL is the length along the sensor FOV that represents the distance across the cloud. The C part of CL is the average concentration along that pathlength. There is an exponential relationship between the CL and the FGC transmission:

$$\tau = \exp(-a \text{CL}) \quad (3)$$

where  $a$  is the absorption coefficient in  $\text{m}^2/\text{mg}$ , and CL in units of  $\text{mg}/\text{m}^2$  is the concentration in  $\text{mg}/\text{m}^3$  times the pathlength in m. The absorption coefficient spectrum may contain a single peak or many peaks depending on the gas. The  $a\text{CL}$  product is referred to as the absorbance.

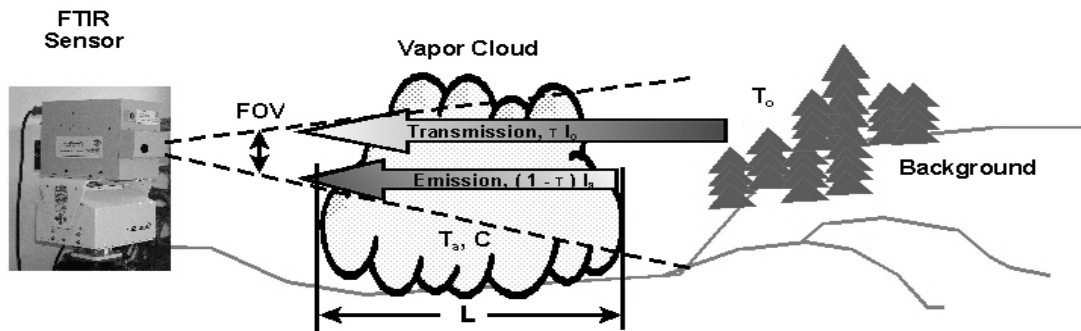


Fig. 2 – Passive FTIR sensor FGC signal model.

## 2.5 Radiometric Calibration

Radiometric spectra in known units are required to produce quantitative results with passive FTIR. The FTIR self radiance and detector response must be removed in order to obtain radiometric spectra. MESH developed a non-linear, multi-point calibration method based on a modified version of a method suggested in the literature [3]. Due to instrument drift, frequent calibration via the automated blackbody source is required. The temperature range of the blackbody set is automatically chosen to best bracket the scene within the limits of the blackbody operation. Typically, the calibration range is +/-15K from ambient temperature.

## 2.6 Detection Algorithm

The proprietary MESH 15 detection algorithm processes each igrm individually by removing the background, performing pattern recognition on the preprocessed spectrum, and then detecting/identifying any FGC of interest that is present in the spectrum. The igrm is then processed with the quantitative algorithm to obtain a CL result.

## 2.7 Quantitative CL Measurement Algorithm

The quantitative algorithm steps include:

1. Use the radiometric calibration to convert the igrm to the scene radiance spectrum,
2. Convert the radiance spectrum to a brightness temperature spectrum via the inverse Planck function,
3. Use the brightness spectrum to determine the effective background temperature and the gas temperature, and
4. Solve for the CL value of the gas identified by the MESH 15 detection algorithm, if the FGC of interest is detected, otherwise the CL result is zero.

The brightness temperature spectrum is the apparent temperature of the radiance for each wavenumber bin assuming that the radiance came from a blackbody source. The gas temperature may also be supplied by the user via an option in the CCTS software.

The background and gas temperatures along with the foreign gas spectral absorption or emission feature radiance,  $I$ , are used to solve for the CL result:

$$CL = -\text{Ln} [(I - I_a) / (I_o - I_a)] / a \quad (4)$$

The background and ambient radiance terms in equation 4 can be determined using the Planck function with the appropriate temperature and wavenumber values. The absorption coefficient spectrum must be convolved with a sinc function to match the FTIR resolution before it is used in equation 4.

The FTIRBox CL measurement uncertainty was measured with a gas cell containing a constant CL challenge of 1,1,1,2 tetrafluoroethane. The CL uncertainty is a function of temperature difference and absorbance peak magnitude. The CL uncertainty is +/-25% @  $|\Delta T|=3K$  and +/-10% @  $|\Delta T|=15K$  for a ~0.6 absorbance unit spectral peak magnitude. These uncertainty values are primarily due to the FTIR noise and background temperature measurement error. They do not include the error in determining the gas temperature.

## 2.8 Tomography Algorithm

The CL results as a function of azimuth from each horizontally scanning FTIRBox are collected in the user interface and display command post computer and then processed by a 2D tomography algorithm to produce cloud maps. The 1 km x 1 km truth box is divided into a 20 x 20 grid. A concentration result is obtained for each 50 m square grid cell via the following steps:

1. Determine the grid cells that contain the FGC. This is done using simple geometry to determine the intersection of the non-zero CL vectors and the grid cells. At least two non-zero CL results from different FTIRBoxes are required to identify a grid cell as containing the foreign gas. A binary cloud map, i.e. a two color plot, can be created with the results of identifying the truth box grid cells with zero and non-zero concentrations. The binary map shows the FGC size and location.
2. The binary cloud map data and the CL vectors are the input to the algebraic reconstruction technique (ART) tomography algorithm. The binary map constrains the tomography algorithm so that it converges on a solution faster. The ART algorithm produces an average concentration result for each grid cell. The grid cell results are used to plot the FGC concentration map.

There are additional results that are calculated with the cloud maps including the cloud centroid, the cloud mass per unit thickness, the cloud size, and the cloud perimeter.

The ART was selected after reviewing several different tomography techniques because the ART performs well with noisy input data [4]. CL results from passive FTIR at low temperature contrast are inherently noisy.

## 2.9 Cloud Height Calculation

A single vertically scanning FTIRBox monitors the cloud height. The FTIR in this FTIRBox has a 0.5 degree FOV. The cloud height is determined by solving a triangle consisting of the vertically scanning FTIRBox location, the FTIRBox maximum detection elevation angle, and the cloud centroid location. The cloud height is measured along a vector perpendicular to the wind direction that passes through the center of the truth box.

## 3 SYNCHRONIZED DATA COLLECTION OF GAS RELEASES

The CCTS was operated for 10 hours a day for approximately 6 months of duration during the last 2 years to monitor various acetic acid (AA), triethylphosphate (TEP), and sulfur hexafluoride (SF<sub>6</sub>) FGC releases. The goal was to determine the cloud size and position as a function of time as the cloud moved through the truth box. The CCTS operator in the command post would setup the scan patterns for the FTIRBoxes and then initiate data collection just prior to the release. Most of the time, the CCTS plotted maps of the cloud in real time as the cloud moved through the truth box, depending on weather conditions and the quality of the FGC release.

### 3.1 FGC Releases

The CCTS has been used to record both stack and explosive type releases through the truth box at Dugway Proving Ground. The stack releases are usually disseminated from 3 heated stacks that exhaust ~10m above ground level and are ~50m apart from each other. The stacks are 250m upwind from the edge of the 1 km x 1 km truth box. A typical duration for a stack release was 30-60 seconds.

The explosive release is preferred for disseminating flammable liquid chemicals contained in plastic jugs. A layer of dirt between the explosives and the chemical jugs prevents the chemical from igniting. The explosive releases were positioned along the leading edge of the truth box. The explosive releases were usually organized into 3 sets of 5 second delayed charges to form a large FGC.

### 3.2 Scanning the Truth Box

All scanning FTIR units are controlled from a single laptop PC in a command post. The CCTS software displays status information for each FTIRBox, real-time spectra from any desired FTIRBox, and map results, as shown in the CCTS diagram in Figure 3. The FTIRBoxes on the truth box corners scanned a 90 degree azimuth range. The vertically scanning FTIRBox typically scanned an elevation range from 0 to +45 degrees at half the speed of the horizontally scanning units. The scanning was synchronized so that all FTIRBoxes started and ended scanning at the same time between map results.

Cloud maps are updated at a rate of 3 times per minute. The mapping cycle consists of 12 seconds to scan the truth box, 2 seconds to process the CL results from each FTIR with the tomography algorithm, and 6 seconds to display the resulting map. The FTIR units calibrate concurrently with the tomography processing and map display steps of the cycle. The detection vectors from each FTIRBox are drawn on the map display in real-time during the scanning of the truth box. A typical set of detection vectors is shown in Figure 4.

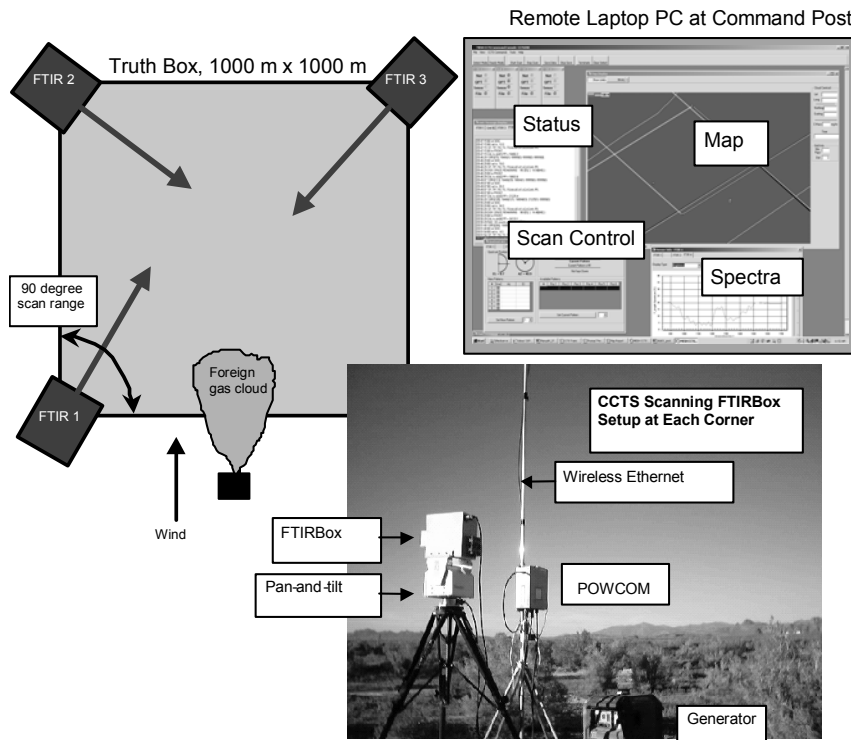


Fig. 3 – CCTS diagram including equipment setup and command post software display.

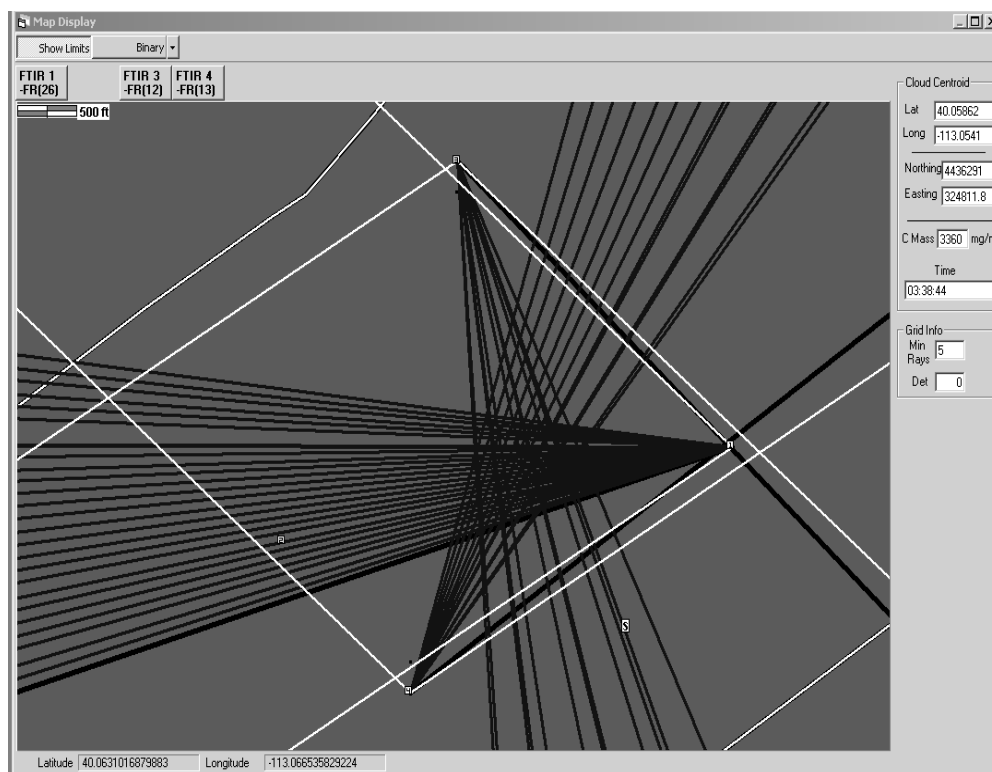


Fig. 4 – A typical set of CL measurement vectors from 3 FTIRBoxes after scanning the truth box.

#### 4 TYPICAL CCTS FGC RESULTS

Data from typical FGC releases are presented. Typical brightness temperature spectra, a CL plot as a function of azimuth, and a cloud map sequence are presented.

##### 4.1 Brightness Temperature Spectra

Spectra from an SF<sub>6</sub> release with a low angle sky background are shown in Figure 5. The SF<sub>6</sub> gas spectral feature is visible in emission at 945 cm<sup>-1</sup>. Note that the background and SF<sub>6</sub> spectra agree everywhere except in the vicinity of the SF<sub>6</sub> peak location. The doublet peak structure between 1000 and 1100 cm<sup>-1</sup> is due to ozone. The ambient air temperature is approximately 10°C, and the brightness temperature is close to this level at either end of the spectrum where the air is less transparent due to water vapor and carbon dioxide. The SF<sub>6</sub> feature is located in a high transmission region for the atmosphere where the FTIR can ‘see’ further into the cold sky, which explains the low brightness temperature background level between 900 and 1000 cm<sup>-1</sup>.

An AA brightness temperature spectrum is shown in Figure 6. The AA’s broad primary and secondary features are also shown in emission against a low angle sky background between 900-1000 cm<sup>-1</sup> and between 1100 and 1200 cm<sup>-1</sup>.

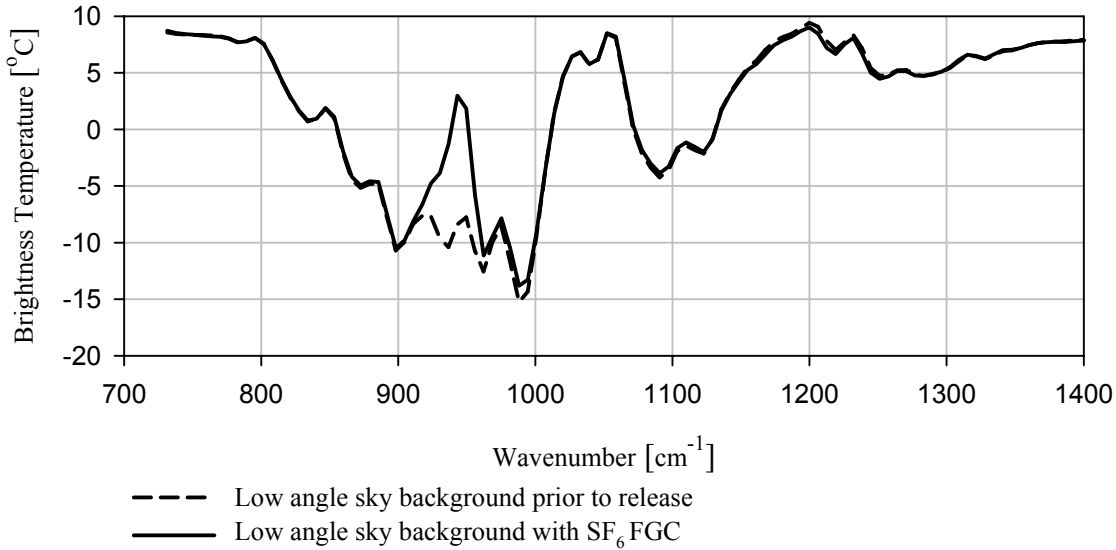


Fig. 5 – SF<sub>6</sub> FGC release brightness temperature spectra.

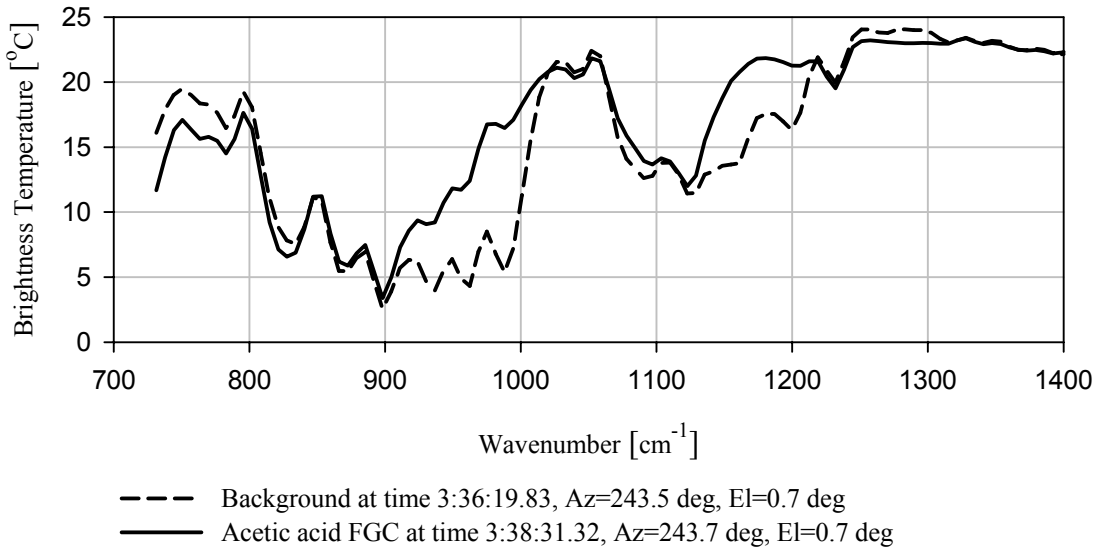


Fig. 6 – AA FGC release brightness temperature spectra.

**4.2 CL as a Function of Azimuth**

A typical CL profile from an AA cloud is shown in Figure 7. As expected, the FGC CL has a rising edge, a high CL region, and a falling edge as the FTIRBox scans across it. Note that there were 2 missed detections near an azimuth of 180-185 degrees. These are usually caused by a bad igrm. The slightly uneven spacing between CL data points is due to a +/- 1 to 2 deg error in reading the Quickset scanner azimuth scale due to communication time lag between the scanner and the

embedded FTIRBox computer. The typical pathlength across this AA FGC was 500 m, which means that the maximum average AA gas concentration along the path was  $2.4 \text{ mg/m}^3$ .

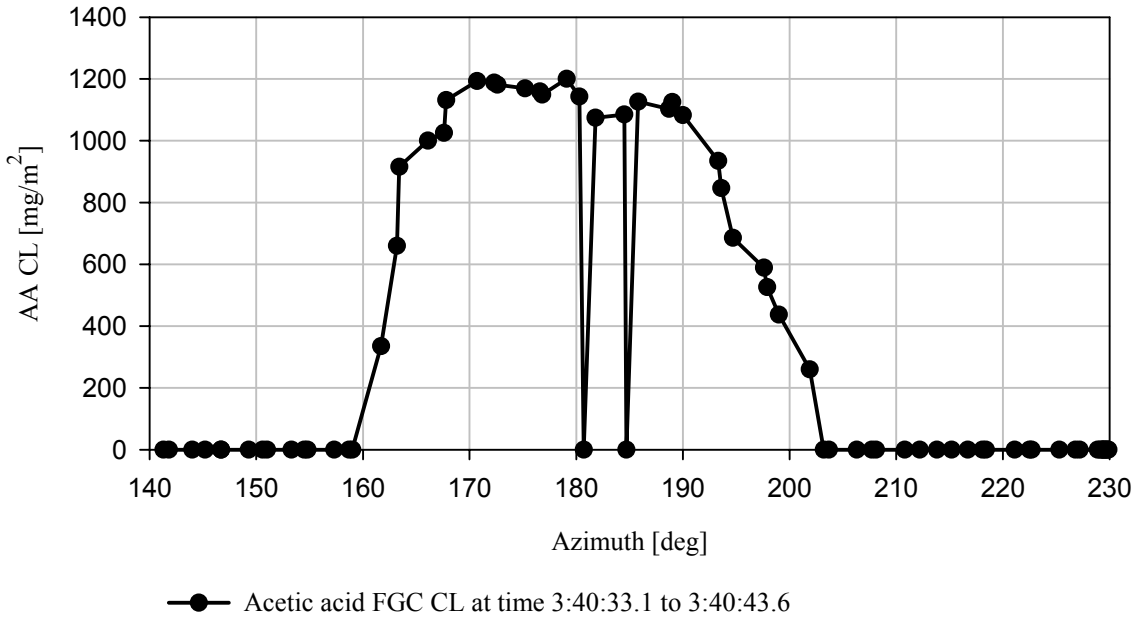


Fig. 7 – Typical CL AA FGC profile as a function of azimuth.

### 4.3 Cloud Map Sequence

A typical partial binary cloud map sequence is shown in Figure 8. The FGC is shown entering and moving through the truth box over a 2 minute time period.

The cloud map results were used to determine the cloud size as a function of time:

Map	Time	Height[m]	Length[m]	Width[m]
1	03:38:44		250	100
2	03:39:04		300	250
3	03:39:24	52	400	350
4	03:39:44	39	450	400
5	03:40:04	26	550	450
6	03:40:24	19	550	450
7	03:40:44	16	550	450
8	03:41:04	1	550	400
9	03:41:24		450	350
10	03:41:44		300	200
11	03:42:04		150	100

The cloud size measurement resolution is limited to the grid resolution of 50 m. The cloud height is only reported as the FGC crosses the centerline of the truth box. Note that the maximum height of the gas cloud occurred at the leading edge. The height accuracy is limited by the FOV spot size which is 4.4 m in diameter at a distance of 500 m.

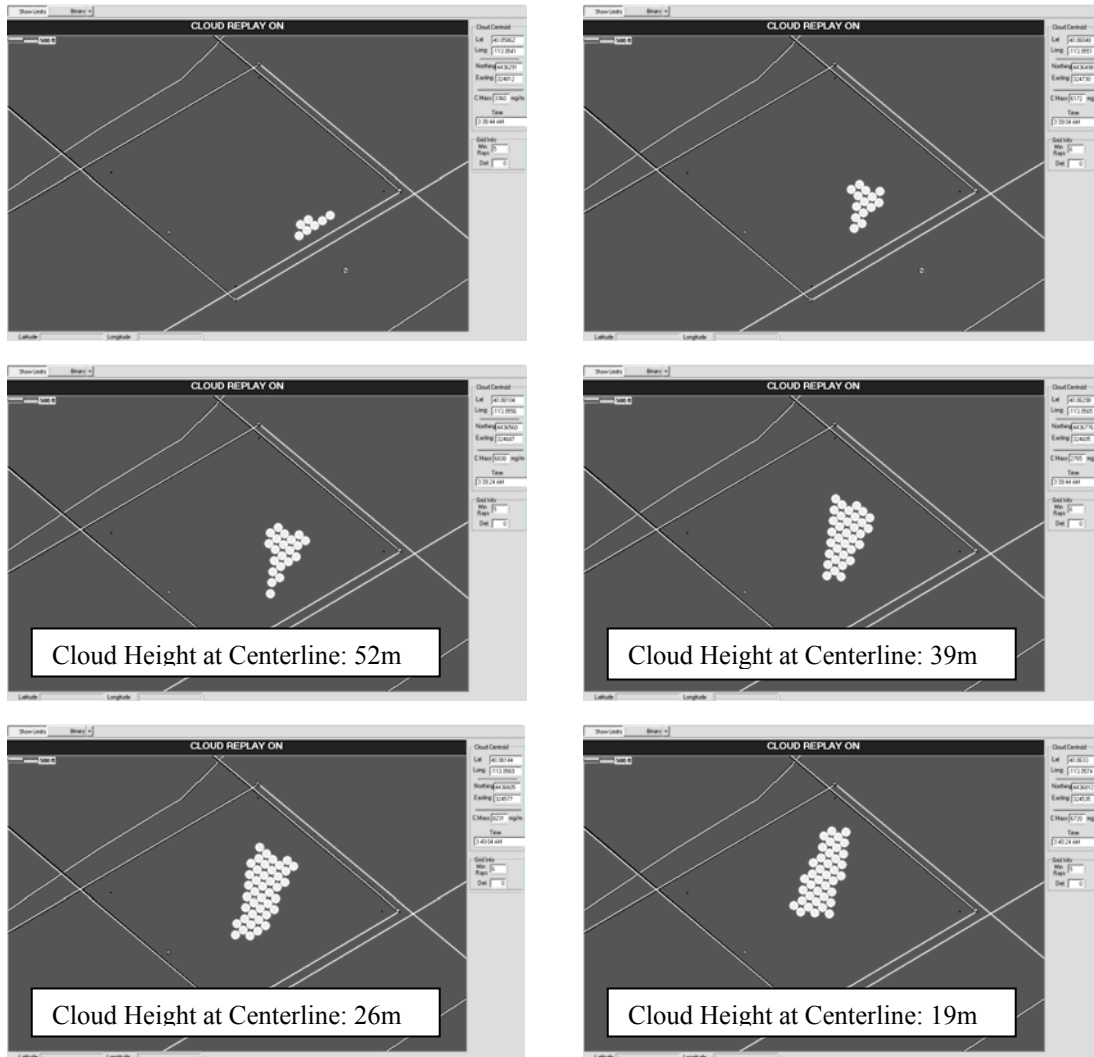


Fig. 8 – Partial AA binary cloud map sequence from time 3:38:44 to 3:40:24.

## 5 FUTURE CCTS R&D

Future CCTS R&D includes design for faster mapping rates, improved tomography, characterization of the concentration map uncertainty, and 3D tomography. These areas of R&D will improve the next generation CCTS.

## REFERENCES

1. Griffiths P and deHaseth J. *Fourier transform infrared spectrometry*. 1st edition, John Wiley and Sons, 1986.
2. Siegal R and Howell J. *Thermal radiation heat transfer*. 3rd edition, Hemisphere Publishing Corporation, 1992.
3. Revercomb H, Buijs H, Howell B, LaPorte D, Smith L and Sromovsky L. Radiometric calibration of IR fourier transform spectrometers: Solution to a Problem with the High-Resolution Interferometer Sounder. *Applied Optics*, Vol. 27, No. 15, 1988.
4. Verhoeven D. Limited-data computer tomography algorithms for the physical sciences. *Applied Optics*, Vol. 32, No. 20, pp 3736-3754, 1993.